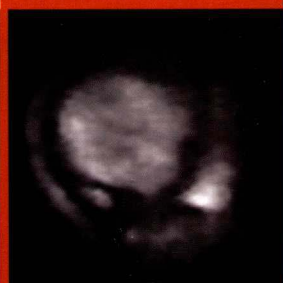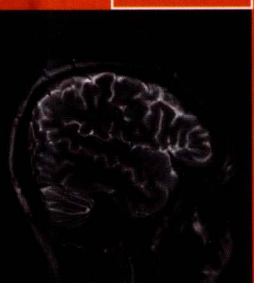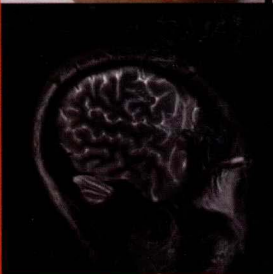Robert H. Kraus Jr.

Michelle A. Espy

Per E. Magnelind

Petr L. Volegov

ULTRA-LOW FIELD NUCLEAR MAGNETIC RESONANCE

A NEW MRI REGIME

OXFORD

ULTRA-LOW FIELD NUCLEAR MAGNETIC RESONANCE

A New MRI Regime

Robert H. Kraus Jr., PhD
Chief Scientist, Samitaur Medical Technologies

Honolulu, HI

Michelle A. Espy, PhD
Scientist, Los Alamos National Laboratory

Los Alamos, NM

Per E. Magnelind, PhD
Scientist, Los Alamos National Laboratory

Los Alamos, NM

Petr L. Volegov, PhD
Scientist, Los Alamos National Laboratory

Los Alamos, NM

OXFORD
UNIVERSITY PRESS

ULTRA-LOW FIELD NUCLEAR MAGNETIC RESONANCE

A New MRI Regime

Robert H. Kraus Jr., PhD
Chief Scientist, Samsung Medical Technologies
Honolulu, HI

Michelle A. Espy, PhD
Scientist, Los Alamos National Laboratory
Los Alamos, NM

Per E. Magnelind, PhD
Scientist, Los Alamos National Laboratory
Los Alamos, NM

Petr L. Volegov, PhD
Scientist, Los Alamos National Laboratory
Los Alamos, NM

OXFORD

To those who, through science, would help others.

FOREWORD

A decade ago in Berkeley, it was shown that the nuclear magnetic resonance (NMR) line width of protons in a liquid could be very narrow in a magnetic field B_0 of a couple of microtesla, even though it was deliberately made highly inhomogeneous by the standards of conventional NMR. In fact, the narrow line width was to nobody's surprise; the important point being the high signal-to-noise ratio (SNR) obtained at a Larmor frequency f_0 of 75Hz. This was achieved by combining two well-known ideas: pre-polarization of the proton spins by a much larger magnetic field B_p that was turned off before the NMR signal was acquired, and the detection of the NMR signal with an untuned detector based on a superconducting quantum interference device (SQUID). Most SQUIDs operate at 4.2K, the boiling point of liquid helium. Unlike a Faraday detector, the SQUID has a frequency-independent response to magnetic flux. These early experiments also demonstrated the simplicity of obtaining the spectra of two nuclear species in a single acquisition using switched magnetic fields and of directly detecting the scalar coupling (J-coupling) splitting in heteronuclear spin systems—a unique benefit of the SQUID sensor.

Subsequently, the Berkeley group made the logical step to ULF magnetic resonance imaging (ULF MRI) by adding switched field gradients. Their system, built with lumber and copper wire coils, operated in a magnetic field of 132μT, corresponding to $f_0 = 5,600$Hz, four orders of magnitude lower than in conventional high-field (HF) MRI. The first image was of a pepper slice. Shortly after, an in-plane resolution of 1mm was demonstrated. This was followed by the three-dimensional *in vivo* image of an arm with an in-plane resolution of 2mm. Subsequently, the group demonstrated the strong dependence of the longitudinal relaxation time T_1 on the concentration of agarose gel in water at low fields, in contrast to the weak dependence at high fields. This observation resulted in the development of ULF T_1-weighted contrast imaging. The large skin depth of metals at ULF enabled the imaging of a pepper in a metal container. The requirement of only modest field homogeneity at ULF made possible undistorted images in the presence of a metal bar, which could, for example, be an orthopaedic screw.

Today, groups at perhaps 20 institutions worldwide are involved in some aspect of ULF NMR and ULF MRI. For example, a line width of 0.034Hz was observed in benzene in the Earth's field, and of 0.34Hz in a J-coupling spectrum. An early demonstration was the simultaneous acquisition of the stimulated magnetic signal from the human brain (magnetoencephalography [MEG]) and the ULF NMR signal from protons in the brain, using a single SQUID. Although these signals were in no way correlated, this was an important demonstration of the potential to combine the two modalities into a single acquisition system. Three-dimensional *in vivo* images of the brain were acquired with multiple SQUIDs. Trials at the Albuquerque airport showed the ability of ULF MRI in a T_1-contrast imaging

mode to seek out liquids in carry-on luggage. On the technical front, an MRI phantom was successfully imaged using a SQUID on a cryocooler. Alternative sensors to SQUIDs are being explored—for example, "mixed sensors," which combine a superconducting pickup loop with a giant magnetoresistance sensor, and atomic magnetometers.

What are the long-term prospects for this field? In my view, although other as-yet-unheralded applications will undoubtedly emerge, if there is to be a major application it will be in medical imaging. But it will not be easy! HF clinical MRI is a magnificent tool, with perhaps 30,000 machines worldwide. Its great versatility leads to multiple applications, and it can achieve a spatial resolution of 1mm for most parts of the human body in a relative short time. A particular advantage is that specifically designed detection coils—at room temperature—can be placed over any part of the body to optimize detection sensitivity.

What would it take for ULF MRI to compete? It's mostly a question of SNR. The magnetic moment of a given ensemble of spins scales as B_0, and the signal it induces in a tuned pickup coil—by Faraday's law—scales as f_0. Thus, all things being equal, the signal from a tuned detector scales as B_0^2. Given that realizable pulsed pre-polarizing fields are likely to be an order of magnitude lower than the 1.5T field of a clinical system and that ULF MRI involves an untuned detector, the simple fact is that ULF MRI is unlikely to compete with HF MRI in terms of combined speed and spatial resolution. One may argue, with some justification, that a ULF MRI machine is likely to be substantially less costly than a 1.5T machine, but at least in the developed world the radiologist—not to mention the patient—seeks high resolution without an unduly long imaging time. Thus, in my view, if the goal of ULF MRI is to compete head on with HF MRI on its own terms, it is doomed to failure.

Fortunately, ULF MRI has its own virtues that extend beyond raw speed and resolution. An obvious strength is its greatly enhanced T_1 contrast compared with HF MRI. In HF MRI, T_1-weighted contrast imaging is well established but has its limitations. For example, in the case of breast cancer, there is no intrinsic T_1 contrast between cancerous and healthy tissue. This drawback is overcome by injecting a Gd-salt into the bloodstream, which flows preferentially to the tumor. The paramagnetic Gd ions enhance the T_1 relaxation rate, enabling one to image the tumor. Although this technique yields high resolution of the tumor, the rate of false positives has inhibited its becoming a screening technique for breast cancer. The use of the contrast agent works well for brain tumors but not at all for prostate cancer, which is the second leading cause of cancer deaths among American men.

The intrinsic difference in T_1 at low fields for different tissue types has been long known; it is the development of ULF MRI that has enabled one to take advantage of it. Although ULF T_1-weighted contrast imaging is well established in phantoms, in tissue it is in its infancy. Studies at Berkeley on *ex vivo* prostate tissue surgically removed from cancer patients, however, have established that T_1 in tumors is substantially shorter than in normal tissue. Simulations suggest that this T_1 difference is sufficient to produce *in vivo* images with sufficient contrast-to-noise ratio and spatial resolution to be clinically significant. Clearly, only clinical trials can establish the effectiveness of this technique, which relies on the intrinsic difference of T_1. If it were possible to image prostate cancer with ULF MRI, one could hope to use it, for example, to assess the extent of the disease in newly diagnosed patients, to provide a map to guide biopsy should it be deemed necessary, and to monitor changes in the prostate during active surveillance or therapies such as brachytherapy (implantation of radioactive seeds), thereby obviating the need for repeated biopsies. An obvious question is the applicability to other kinds of cancer. Could ULF MRI be used to screen for breast cancer? Or to detect ovarian cancer—which is notoriously difficult to detect at an early stage? Again, only clinical trials can address these questions.

A second forward-looking application of ULF MRI is its combination with systems for MEG. These systems, containing typically 300 SQUIDs, are used to detect stimulated or spontaneous magnetic fields from neurons in the brain in real time. They are used, for example, for presurgical mapping of brain tumors, the locating and presurgical mapping of sites of focal epilepsy, and the progression of recovery from brain trauma such as brain injury or stroke. To interpret the magnetic source image, an MRI of the brain is essential. The MEGMRI project, funded by the European Union and involving about a dozen institutes led by Aalto University, Helsinki, aims to incorporate ULF MRI into MEG systems. In principle, this simply involves the addition of appropriate sets of coils to existing MEG systems. The NMR signals are detected by the array of SQUIDs, so that averaging over these sensors can substantially reduce their noise. The notion of obtaining magnetic source and MR images with a single system is very appealing, since it overcomes difficulties in co-registering images obtained with two different systems and could result in substantial cost savings. In practice, the combination of MEG and MRI has many challenges, but there is every reason to believe these will be overcome. If so, these combined technologies could have a significant impact both clinically and commercially.

Currently, the holy grail of ULF MRI is its potential for direct neural current imaging (DNI). The essential idea is that currents flowing in neurons during neural activity produce local magnetic fields that can induce a tiny shift in the phase of the NMR signal over a tiny region. Strenuous efforts have been expended to observe this effect in HF MRI, so far without success. Since ULF MRI operates at a magnetic field four orders of magnitude lower, one expects the relative shift of the NMR signal to be enhanced by the same factor. The realization of DNI would be revolutionary, making real-time, spatially localized observation of neural activity a reality.

What are the challenges in bringing ULF MRI to clinical practice? The single biggest issue is, again, SNR, which scales as the ratio of the NMR signal at the sensor to the noise at the sensor, B_N. The imaging time for a given spatial resolution sales inversely as $(SNR)^2$, and hence as B_N^2/B_P^2. This immutable law should be displayed prominently in every ULF MRI laboratory! To obtain a sensible imaging time, one requires a sensor noise approaching $0.1\ fTHz^{-1/2}$ (roughly the limit set by body noise) and a polarizing field of at least 0.1T. Both are achievable, but not trivially. A noise of $0.1\ fTHz^{-1/2}$ is at the limit of what one can detect with an appropriate coil size and a SQUID at 4.2K, and assumes that environmental noise can be reduced to this level. Generating a pulsed magnetic field of, say, 0.15T at the prostate or head that can be turned off in some milliseconds is achievable but requires a water-cooled coil and a power supply providing at least 50kW. Screening out external electrical and magnetic interference, almost certainly with a shielded room, presents a major challenge. When the polarizing field is switched off, large eddy currents in the room can severely distort both B_0 and pulsed gradient fields unless one either cancels the field with a second, counter-wound coil or designs a room that rapidly damps out low-frequency current while retaining a high degree of screening at the imaging frequency. Perseverance by the community will undoubtedly achieve these goals.

Another issue concerns cryogenics. I believe the clinical community is unlikely to embrace a system that requires refilling with liquid helium every few days. Fortunately, reliable cryocoolers are readily available at reasonable cost, and ULF MRI has already been demonstrated with a cryocooled SQUID. An alternative approach would be a refrigerator that automatically refills the cryostat at night.

Finally, one should not underestimate the time and cost required for clinical trials. To undertake a meaningful trial will require a company with deep pockets and, one hopes, a steady stream of federal funding.

The group at Los Alamos National Laboratory has been a major driving force in the development of ULF MRI. Their efforts are reflected in this book, which covers all aspects of the subject in depth, ranging from history and the nuts-and-bolts practicalities of building such a system to ULF resonance phenomena and applications of a variety of imaging techniques to pulse sequences and direct neural current imaging. The book is surely destined to become the standard reference in the field.

John Clarke
Berkeley
May 12, 2011

PREFACE

This book endeavors to provide the background for and current status of the emerging field of ultra-low field (ULF) magnetic resonance imaging (MRI). We lay the groundwork by providing a brief history of MRI at extremely low fields and for why ULF NMR and MRI are of both scientific and practical interest. In particular, we examine the benefits realized at applied magnetic fields that are many orders of magnitude below traditional NMR and MRI. We balance the benefits at ULF with the various anticipated and unanticipated challenges our team and others working in the field have experienced, and a variety of approaches used to deal with these challenges. We present the current status in sufficient detail for the reader to effectively pursue ULF MRI investigations in both medical and material science applications. While the primary focus of this book is MRI, we discuss a variety of nuclear magnetic resonance (NMR) phenomena, particularly as they apply at ULF, because ultimately MRI is simply a spatially encoded measurement of specific NMR phenomena.

Traditional MRI involves applied magnetic fields typically in the Tesla regime. Most clinical imaging instrumentation operates at 1.5T, with more 3T imagers being installed every day. The lowest magnetic fields commonly used in clinical instruments are 0.3T (3kG) in applications where an open geometry is required and lower spatial resolution is acceptable or tolerable. Exploring NMR signals at extremely low fields in the milli-Tesla regime was initially reported about two decades ago, where the NMR signal for water was observed at 10mT. However, it has been only in the last decade or so since the observation of exceptionally narrow NMR line widths for various liquid solutions at a few micro-Tesla was reported. The field of ULF NMR and MRI has seen a tremendous growth of publications and research investment around the world since then. This book describes the current state of the art of ULF MRI in our laboratory and others, and while we make an effort to be thorough and relatively complete, the field is evolving rapidly and new ideas are constantly being pursued and reported. We will share practical insights into ideas being pursued and conclude the book with a number of promising concepts for ULF applications that have yet to be investigated and are, as yet, unproven.

Our book focuses on the practical aspects of ULF MRI that will enable the reader to practice in the field. Only a few of the most relevant derivations of first principles of ULF NMR and MRI are provided, with a focus on those specifically relevant to the regime of ULF (e.g., concomitant gradients) and those we thought were lacking elsewhere. Others are provided in the bibliography. We attempt to present a thorough discussion of concomitant gradients because of the large effect they can have on MRI at ULF. While they have been mentioned in high field MRI texts, concomitant gradients have been either treated with simple approximations or entirely ignored.

We present a detailed discussion of current state-of-the-art instrumentation that is unique to ULF MRI. The most common sensor to acquire the NMR signal for ULF MRI is the superconducting quantum interference device (SQUID). SQUIDs are the most sensitive magnetic field sensors in wide use today but require cooling with liquid cryogens (liquid nitrogen or liquid helium). Furthermore, SQUIDs require extraordinary expertise and measures to operate in a typical ULF MRI environment. While we thoroughly cover the techniques needed to employ SQUID sensors in ULF MRI, we also discuss the ongoing search for robust, noncryogenic sensors with the required sensitivity to the desired signal. We present the tradeoffs for currently available sensors. Our discussion of the instrumentation also includes all other aspects of the hardware used in ULF MRI systems, together with experimental techniques and practical insights into how it all works.

We have interspersed relatively general material throughout the book to provide a complete and self-consistent picture for the reader, but we also rely heavily on many excellent references and readily available sources as needed to provide a comprehensive picture of the field. We have made an effort to carefully define nomenclature and thoroughly describe methods to avoid the confusion that can occur between the many sources of NMR information, particularly as one switches between high-field and ULF MRI. A comprehensive table of acronyms and abbreviations is also provided.

Working at the forefront of a new field is exhilarating, educational, and competitive. Many novel features and capabilities of ULF MRI have been discovered, yet we are certain that only the proverbial surface of the field has been scratched. There is far more yet to be discovered and learned, and we wish you, the reader, the very best of luck and insight.

Robert H. Kraus Jr.
Michelle A. Espy
Per E. Magnelind
Petr L. Volegov

ACKNOWLEDGMENTS

COMMON ACRONYMS AND ABBREVIATIONS

We include a list of common acronyms, abbreviations, and symbols used in this book. We ask the reader to be aware that sections of the book where detailed mathematical derivations are presented may use symbols and letters in formulae that are not consistent with this table. We have, however, attempted to clearly define every symbol and character at the first instance of use in the context of the derivation.

2D	Two-dimensional
3D	Three-dimensional
A	Context dependent: Amp or Nuclear mass number (number of protons and neutrons in a given nucleus)
Å	Ångström, 10^{-10}m
AC	Alternating current (time-varying current)
ADC	Analog-to-Digital converter
AM	Atomic Magnetometer (or Atomic Magnetometry)
ASL	Arterial spin labeling, a MRI technique used to measure blood flow that can be used to deduce brain function
B_0	MRI magnetic field, typically both the polarization and measurement field used in high-field MRI
B_m	Measurement magnetic field
BOLD	Blood Oxygen Level Dependent, a MRI technique used to deduce brain activity
B_p	Polarization magnetic field used in MRI.
BW	Bandwidth
CNR	Contrast-to-noise ratio
CSF	Cereberal spinal fluid
DC	Direct current (constant current)
DNI	Direct neural imaging, a method to directly measure the neural activity (presumably in the brain). Our team coined the acronym to refer to the direct imaging of neural currents using ULF MR

e	Elementary charge
EEG	Electroencephalography
EIT	Electrical impedance tomography
EPI	Echo-planar imaging
f	Frequency, when used as a variable or quantity, typically in Hz.
FAIR	Flow-sensitive alternating inversion recovery, a MRI technique to used to measure blood flow that may be associated with function
FC	Field cycling, typically refers to techniques for varying the NMR or MR field
FFT	Fourier Transform (or Fast Fourier Transform)
FID	Free Induction Decay
FLAIR	Fluid attenuated inversion recovery
FLASH	Fast low-angle shot
fMRI	Functional magnetic resonance imaging
FOV	Field-of-view, often (thought not always) synonymous with volume of interest
G	(non-italicized) Gauss, unit of magnetic field equal to 10^{-4} T
G	Magnetic field gradient (usually includes a direction: G_x, G_y, G_z).
GMR	Giant magneto-resistive or giant magnetoresistance
h	Planck's constant (6.626×10^{-34} J-sec)
H	Magnetic field strength
$\hbar$	$h/2\pi$ or the reduced Planck's constant (1.055×10^{-34} J-sec)
HF	High Field, typically referring to >0.3 T imaging field in HF MRI
HTC	High (critical temperature) superconductor, typically designates materials with superconducting critical temperature well above ~4 K. also high-T_c
Hz	Hertz, cycles per second
I	Context dependent: Current or spin quantum number
J	Current density
J	(non-italicized) Joule
k	The mathematical space convient for imaging, "k-space"
K	Kelvin
k_B	Boltzmann's constant (1.381×10^{-23} J/K)
L	Inductance (also used as image size in Ch. 4 derivations)
LANL	Los Alamos National Laboratory
LF	Low (magnetic) Field, commonly referring to MRI fields below 0.3T. We define LF MRI as the regime between ULF MRI and HF MRI.
LHe	Liquid helium
LN	Liquid Nitrogen
LSB	Least Significant Bit, the lowest significant bit in a digital acquisition system
LTC	Low (critical temperature) superconductor, typically ~4 K and below. Also low-T_c

M	Magnetization, may be a vector ($\mathbf{M}$) quantity, scalar (M) or a vector component (e.g. M_x)
MAGVIZ	The name given to the ULF MR relaxometry technique used to differentiate materials based on relaxation profile
MEG	Magnetoencephalography
MR	Magnetic Resonance
MREIT	Magnetic Resonance electrical impedance tomography
MRI	Magnetic Resonance Imaging
MSR	Magnetically Shielded Room
N	Number in a given population (such as number of spins)
nc-MRI	Neural current MRI—designates methodologies used in MRI to detect signatures directly associated with neural activity (such as rapid dephasing).
NEMA	National Electrical Manufacturers Association, See also www.nema.org
NMR	Nuclear Magnetic Resonance
NQR	Nuclear quadrupole resonance
PET	Positron emission tomography (medical imaging modality using radioisotopes)
PSD	Power Spectral Density
R	Resistance
Rad	Radian
RF	Radio frequency, often referred to as "rf" elsewhere
RFI	Radio frequency interference
ROI	Region of Interest (see VOI/volume of interest)
S	Context dependent: Shielding factor (various subscripts designate specific type), or the NMR signal measured from a specific region or volume.
SD	Standard deviation
SENSE	Sensitivity Encoding – a method for using multiple sensor to improve imaging speed or signal-to-noise
SMASH	Simultaneous acquisition of spatial harmonics—a method for using multiple sensor to improve imaging speed
SNR	Signal-to-noise ratio
SOC	Streams of commerce, refers to commonly available packaging of commodities
Spin	Quantum mechanical spin, typically referring to nuclear spin in this book
SQUID	Superconducting Quantum Interference Device
T	(non-italicized), Tesla, unit of magnetic field equal to 10,000 G
T	Context dependent: Temperature or time when used as a variable
t	Typically refers to a time, often denoted by a subscript (e.g. t_g – time gradient field is applied, t_a – acquisition time, etc.)
T_1	Longitudinal (or spin-lattice) relaxation time
T_2	Transverse (or spin-spin) relaxation time

T_c	Critical temperature, typically referring to the temperature at which a material becomes superconducting
ULF	Ultra-low magnetic field (erroneously "ultra-low frequency")
V	(Context dependent) Voltage or Volume
VOI	Volume of interest, typically the imaging region of interest in MRI
Voxel	Volume element, typically referring to a specific size element from which a signal is derived
Z	(non-italicized) refers to the nuclear atomic number
Z	Impedance
μ_0	Free space permeability
γ	Gyromagnetic ratio (depends on isotope/nucleus)
μ	Relative permeability
μ-metal	Mu-metal, generally refers to any high magnetic permeability material
δ	Skin depth—the thickness of a material needed to reduce a signal by $1/e$
σ	Electrical conductivity
χ	Magnetic susceptibility
Ω	Ohm, measure of resistance
ω	Frequency (general)
ω_L	Larmor Frequency

ULTRA-LOW FIELD NUCLEAR MAGNETIC RESONANCE